Journal Pre-proofs

Non-rigid alignment pipeline applied to human gait signals acquired with optical motion capture systems and inertial sensors

Rubén Soussé, Jorge Verdú, Ricardo Jauregui, Ventura Ferrer-Roca, Simone Balocco

PII:	S0021-9290(19)30676-1
DOI:	https://doi.org/10.1016/j.jbiomech.2019.109429
Reference:	BM 109429

To appear in: *Journal of Biomechanics*

Accepted Date: 13 October 2019

Please cite this article as: R. Soussé, J. Verdú, R. Jauregui, V. Ferrer-Roca, S. Balocco, Non-rigid alignment pipeline applied to human gait signals acquired with optical motion capture systems and inertial sensors, *Journal of Biomechanics* (2019), doi: https://doi.org/10.1016/j.jbiomech.2019.109429

This is a PDF file of an article that has undergone enhancements after acceptance, such as the addition of a cover page and metadata, and formatting for readability, but it is not yet the definitive version of record. This version will undergo additional copyediting, typesetting and review before it is published in its final form, but we are providing this version to give early visibility of the article. Please note that, during the production process, errors may be discovered which could affect the content, and all legal disclaimers that apply to the journal pertain.

© 2019 Published by Elsevier Ltd.

Journal Pre-proofs

Non-rigid alignment pipeline applied to human gait signals acquired with optical motion capture systems and inertial sensors

Rubén Soussé[a], Jorge Verdú[a,b], Ricardo Jauregui[a], Ventura Ferrer-Roca[d], Simone Balocco[b,c]

balocco.simone@gmail.com

[a] *Dycare, Llacuna 162, 08018, Barcelona, Spain*
[b] *Dept. Matematics and Informatics, University of Barcelona, Gran Via 585, 08007 Barcelona, Spain*
[c] *Computer Vision Center, 08193 Bellaterra, Spain*
[d] *Centre Alt Rendiment, Sant Cugat, Spain*

Abstract

An accurate gait characterization is fundamental for diagnosis and treatment in both clinical and sportive fields. Although several devices allow such measurements, the performance comparison between the acquired signals may be a challenging task.

A novel pipeline for the accurate non-rigid alignment of gait signals is proposed. In this paper, the measurements of Inertial Measurement Units (IMU) and Optical Motion Capture Systems (OMCAP) are aligned using a modified version of the Dynamic Time Warping (DTW) algorithm. The differences between the two acquisitions are evaluated using both global (RMSE, Correlation Coefficient (CC)) and local (Statistical Parametric Mapping (SPM)) metrics.

The method is applied to a data-set obtained measuring the gait of ten healthy subjects walking on a treadmill at three different gait paces. Results show a global bias between the signal acquisition of 0.05º.

Regarding the global metrics, a mean RMSE value of 2.65° (0.73°) and an average CC value of 0.99 (0.01) were obtained. The SPM profile shows, in each gait cycle phase, the percentage of cases when two curves are statistically identical and reaches an average of 48% (22%).

Keywords: Inertial Measurement Units, Dynamic Time Warping, Statistical Parametric Mapping, Optical Motion Capture Systems

1. Introduction

Gait characterization is an essential part of both clinical evaluation (e.g. neuro-musculoskeletal disorders (Paquet et al., 2003) and gait abnormalities (Koller and Trimble, 1985)) and improvement of sport performance (Tao et al.,

Journal Pre-proofs

2012). In particular, the knee motion can be acquired along three axes: flexion/extension, abduction/adduction and rotation (internal/external). Nevertheless, for straight walking and running motions, the amplitude of variation of the last two angles usually keeps confined inside a 10° range (Seel et al., 2014). Specifically, flexion/extension knee angle is commonly defined as the difference in inclination between the thigh and shank (Vanrenterghem et al., 2010).

Nowadays, optical motion capture systems (OMCAP) are the gold standard techniques for gait characterization. These systems use reflective spherical markers that are tracked by multiple video cameras from different angles in order to measure body movements. However, the main constraints of such systems are the need of experimental laboratories and complex experimental setup. To overcome these drawbacks, new measurement devices based on inertial measurement units (IMU) equipped with tri-axial accelerometers, gyroscopes and magnetometers, aroused in the market. However, they suffer some limitations: firstly, integrating the angular rates of the gyroscope results in an error drift in the measurement. In addition, it is difficult to place the sensors accurately on the joint axis (Seel et al., 2014).

The literature offers multiple studies in which the measurement error between OMCAP and IMU are evaluated (Seel et al., 2014). In (Takeda et al., 2009) the segment orientation is estimated from the translational and gravitational accelerations obtained by the gyroscope and accelerometer. In (Castañeda et al., 2017), an Euler-based fusion algorithm combining accelerations, angular velocities and magnetic signals is implemented to estimate the sensors orientation. In (Watanabe et al., 2011), uses a Kalman filter to estimate orientation from accelerometer and gyroscope signals. The latter methodology can also be improved taking profit of kinematic constraints of the joint, providing more accuracy (Cooper et al., 2009). Finally, in other studies, pre-calibration methods are utilized to perform the sensor-to-segment transformation (Favre et al., 2008; Noort et al., 2013).

Some clinical scenarios, require the comparison of time-series acquired from different kinematic systems. As an example, the gait pattern comparison before and after a surgical intervention (Knoll et al., 2004) is a common issue. In other cases, the classification of some pathology may require a comparison of the acquired signals against the reference curve of healthy subjects. Indeed, the temporal distortions that may be present in the compared signals, limit the clinic performance in diagnosis and treatment planning (Dobson et al., 2007). To overcome these problems, the acquired signals must be aligned in a common frame. Some authors, do not mention which alignment method was applied in their studies (Takeda et al., 2009; Watanabe et al., 2011; Noort et al., 2013). Others, decide to use rigid methods as initial synchronization, axis alignment or cross-correlation analysis (Favre et al., 2008; Cooper et al., 2009; Castañeda et al., 2017; Seel et al., 2014). When comparing two time series having the same length, if the phases of the signals are not aligned, the matching will not be locally reliable. In other fields or applications, non-rigid matching methods have been proposed. In (Sessa et al., 2013), A Dynamic Time Warping (DTW) algorithm is applied to align IMU and cameras signals in a robotic arm. In

Journal Pre-proofs

(Zhou et al., 2014), DTW is used for human gesture tracking and recognition.

To quantify the differences between two signals, most of the studies in the gait analysis domain utilize global metric parameters such as average Root Mean Square Error (RMSE) to measure angular error and bias and/or Pearson's Correlation Coefficient (CC) to measure waveform similarities (Castañeda et al., 2017; Cooper et al., 2009; El-Gohary and McNames, 2015; Engelhard et al., 2015; Favre et al., 2008; Takeda et al., 2009; Seel et al., 2014). The main limitation of only using global metrics is that a small average error along the cycle may not reflect big local errors at some of the cycle phases. Previous studies highlighted the importance of indicating the portion of the gait cycle responsible for this difference (Deluzio et al., 1997). Studies in other biomechanical applications introduce the use of local waveform similarity metric tools as Statistical Parametric Mapping (SPM) for providing a more detailed signal comparison (Robinson et al., 2015), (Pataky et al., 2008).

In order to properly compare IMU and OMCAP measurements, we propose to use, for the first time in the gait kinematic field, a pipeline allowing the non-rigid alignment of the signals based on the DTW algorithm. The metrics used in the valuation are the RMSE, the CC and the SPM which is introduced for the first time in the gait analysis field. In our experiments, ten healthy subjects were recorded while walking on a treadmill at three different gait paces.

2. Method

2.1. Experimental setup

2.1.1. Material

In this study, two IMU sensors produced by DyCare® (Barcelona, Spain), having a sampling frequency of 104.2 Hz, were used for the measurements. Each sensor integrates tri-axis accelerometer, gyroscope and magnetometer. To obtain the joint angle, the row signals are transformed into quaternions using a Madgwick-based fusion algorithm.

The OMCAP device consisted of a 3D system with eight infrared cameras having an image rate of 300 Hz (Proreflex Qualisys Motion Capture System, Qualisys AB, Sweden). The movement of each participant was tracked with spherical reflective markers positioned according to a 6-Degrees-of-Freedom eight segment "Lower Limb and Trunk" (LLT) (Vanrenterghem et al., 2010) (Figure 1). All modeling and analysis were undertaken in Visual3D (Cmotion, Germantown, MD, USA) with segmented data based on Dempster's regression equations and using geometrical volumes to represent. For both OMCAP and IMU acquisitions, only the knee flexion/extension angle was selected and processed, considering the knee as a hinge joint.

To carry out the measurements, ten healthy subjects (27,3 $\pm$ 9.3 years; 1.80 $\pm$ 0.10 m; 73.37 $\pm$ 7.93 Kg) were evaluated in a treadmill at three different gait paces (2km/h, 4km/h and 6km/h).

Following the same sensor placement proposed in other studies (Castañeda et al., 2017; Cooper et al., 2009; El-Gohary and McNames, 2015; Engelhard

Journal Pre-proofs

et al., 2015; Favre et al., 2008; Seel et al., 2014), two IMU sensors were located the thigh and shank using two cluster plates rigidly attached to the body using straps. In the case of the OMCAP system, four spherical markers were located on each cluster plate to ensure co-planar measurements, while the remaining markers were placed on the knee and toes as shown in Figure 1.

The sensor setup utilized to measure the knee flexion-extension angle was designed standing for simplicity. To avoid anatomical measurements or calibration movements as required in some studies (Donovan et al., 2007; Cutti et al., 2010; Ferrari et al., 2010; Roetenberg et al., 2009), the reference sensor was attached laterally to the leg, using the cluster plate to maintain it parallel to the plane of movement, which is an assumption similar to (Favre et al., 2006).

Considering the approximation that such an assumption implies, an alignment between both sensors was performed to reduce the measurement error. At the beginning of each trial, the couple of sensors were aligned by orienting both quaternion to the same angle in space. The change of basis is obtained by multiplying one of the two vectors by the conjugated quaternion that describes the rotation between them. In such way, the relative translation between the two sensors was always co-planar, reducing the assessment of out-of plane measurements.

Both systems tracked the movement of the thigh and shank, measuring the rotation angles along the three degree of freedom independently. The rotation angles of the knee are defined considering the relative orientation of the shank with respect to the local coordinate system of the thigh. Only the flexion-extension plane was extracted and compared between systems, since it corresponds to the plane with the maximum range of movement (Donovan et al., 2007; Cutti et al., 2010; Ferrari et al., 2010; Roetenberg et al., 2009; Favre et al., 2006).

The volunteers were asked to walk for 15-28 gait cycles depending on the exercise speed in order to guarantee the repeatability of the measurement.

2.1.2. Alignment pipeline

The overall experimental design to compare IMU and OMCAP signals is performed in three phases as follows (Figure 2-a):

1. Assessment of gait kinematic using OMCAP and IMU devices.
    (a) Ten volunteers were recorded while walking on a treadmill. From these acquisitions, two data-sets corresponding to OMCAP and IMU time-series are obtained.
    (b) Each pair of signals (OMCAP and IMU) are firstly separated in segments, belonging to separate gait cycles. Such a result is obtained by identifying the minimum peaks of each repetition (Figure 2-b).
2. Signal non-rigid alignment:
    (a) For each signal all the segments were aligned to an average one using the DTW algorithm. For each OMCAP and IMU signal acquisition, an *average stride* cycle and its standard deviation profile are obtained (Figure 2-c).

Journal Pre-proofs

Figure 1: Illustration of the experimental set-up. IMU sensors (2 white boxes) and OMCAP markers (8 gray spheres) were located on the shank and thigh on two cluster plates. Additional spherical markers were also placed on the knee and toe joints.

   (b) Since IMU and OMCAP *average* profiles are not in a common temporal frame, they are compared pair-wise using the DTW.
   (c) Such operations is repeated for each subject and speed acquisition (Figure 2-d (left)).
3. Computation of metrics RMSE, CCa and SPM (Figure 2-d (right))

Journal Pre-proofs

Journal Pre-proofs

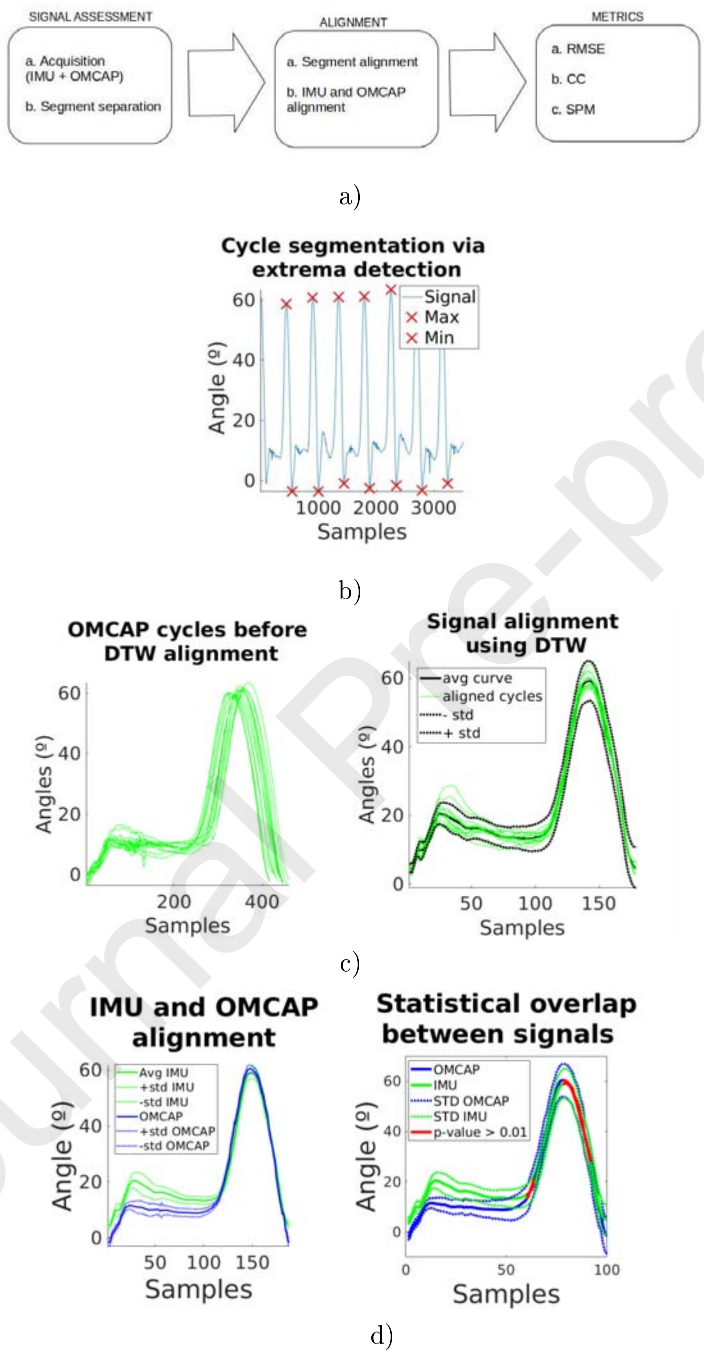

Figure 2: a) General pipeline scheme. b) Stride segmentation by detecting the minimum of each cycle. Red crosses indicating the signal maximum and minimum are superimposed to the blue signal. c) Stride alignment obtained by DTW and average signal computation for each signal. Each gait cycle is represented by a green curve, while a black shape indicates the average curve (solid black) and the corresponding standard deviation (dotted black). d) Left. Alignment between IMU (green) and OMCAP (blue) signals obtained by DTW and example of a SPM assessment. In d) Right, the portion of the signal having statistically similar is depicted in red.

Journal Pre-proofs

Journal Pre-proofs

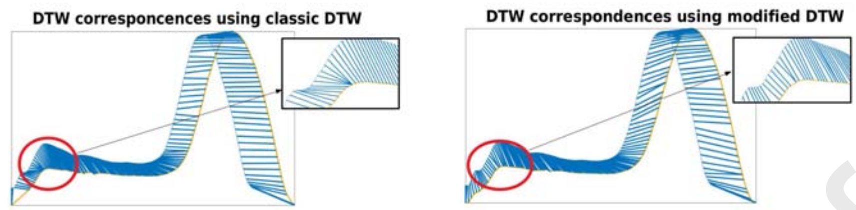

a) b)

Figure 3: Comparison between correspondences generated by classical and improved DTW respectively. As it can be appreciated, the improved DTW allows obtaining a smoother matching between the samples.

2.2. Non-rigid alignment strategy

The DTW is a technique allowing the point-wise synchronization between the samples. The algorithm computates a local cost similarity between the two signals (of n and m the lengths), leading to a cost matrix ($C \in \mathbb{R}^{\mathrm{n} \times \mathrm{m}}$). A warping between the signal is obtained from an accumulated matrix AC in a non-rigid fashion. The classical implementation of the DTW (see (Keogh and Ratanamahatana, 2005)) allows the local alignment but it doesn't guarantee the smoothness and continuity of the synchronization. For instance, multiple correspondences of a single point might appear leading to a non-physiologic behavior (Figure 3-a). In order to improve the DTW algorithm performance, in this specific gait analysis, the following modifications are implemented:

Kernel: The computation of each element of AC is obtained using an improved kernel proposed in (Müller, 2007). Such change, allows to reduce duplicated correspondences between samples.

$$AC(i,j) = C(i,j) + min\{C(i-1-,j-1), C(i-1,j-2), C(i-2,j-1)\} \quad (1)$$

Smoothing: Once computed, the warping path is also smoothed using a Gaussian kernel. This operation reduces the number of consecutive vertical or horizontal samples of the warping path. Figure 3 illustrate how the smoothing of the warping path affect the alignment.

2.3. Comparison metrics

The comparison between the IMU and OMCAP gait signals is performed by computing several metrics, each of them specifically devoted to analyzing a different aspect of the curve alignment. All the metrics are calculated for each subject and exercise speed independently, and subsequently combined to report global results.

The RMSE (Cooper et al., 2009; Cuesta-Vargas et al., 2010; Takeda et al., 2009; Seel et al., 2014; Favre et al., 2008; El-Gohary and McNames, 2015) provides the global distance between two data-sets, computing the average error of the residuals as follows:

Journal Pre-proofs

$$RMSE = \sqrt{\frac{\sum_{t=1}^{N}\left(y_{IMU}(t) - y_{OMCAP}(t)\right)^2}{N}} \tag{2}$$

where y_{OMCAP} is the reference signal (OMCAP) and y_{IMU} is the IMU signal. N is the total number of samples in each average stride, after aligning both signals.

The Correlation coefficient (CC) compare waveform similarity (Watanabe et al., 2011; Takeda et al., 2009; Picerno et al., 2008; Cooper et al., 2009; Favre et al., 2008). The CC is computed as follows:

$$CC = \frac{\sigma_{y_{IMU}y_{OMCAP}}}{\sigma_{y_{IMU}}\sigma_{y_{OMCAP}}} = \frac{\sum_{t=1}^{N} y_{IMU}(t)y_{OMCAP}(t) - N(\overline{y}_{IMU}\overline{y}_{OMCAP})}{\sigma_{y_{IMU}}\sigma_{y_{OMCAP}}} \tag{3}$$

Where: $\sigma_{y_{imu}y_{OMCAP}}$is the covariance of the two measurements, σ_y the variance, $\overline{y}_{IMU}$ and $\overline{y}_{OMCAP}$ the mean signal values.

When conducting statistical tests using time series, statistical parametric mapping (SPM) (J.., 2007) is a technique commonly used to test the null-hypothesis between each pair of samples of the two curves. SPM performs a p-value correction using Random Field Theory to consider the the temporal smoothness of the data (Pataky et al., 2013).

For the purpose of this study, SPM quantifies local waveform similarity through calculating a p-value between IMU and OMCAP in each phase using a two-tailed paired t-test with a p-value=0.01.

3. Results

Table 1 summarizes the computed metrics for every subject and exercise speed, obtained using without DTW, with the classical and with the improved version of the DTW.

		Speed 1 (sp1)			Speed 2 (sp2)			Speed 3 (sp3)		
		RMSE (°)	CC	SPM	RMSE (°)	CC	SPM	RMSE (°)	CC	SPM
Subject 1	no DTW	6.23	0.97	0.14	5.64	0.98	0.22	7.6	0.95	0.2
	DTW classic	4.01	0.99	0.35	4.36	0.99	0.27	2.78	0.99	0.37
	DTW improved	3.82	0.99	0.33	3.05	0.99	0.41	4.04	0.99	0.17
Subject 2	no DTW	2.87	1	0.51	5.85	0.97	0.27	3.43	0.99	0.26
	DTW classic	2.51	1	0.53	3.42	0.99	0.3	3.28	0.99	0.22
	DTW improved	1.9	1	0.61	3.32	0.99	0.34	2.75	0.99	0.34
Subject 3	no DTW	3.07	0.99	0.71	3.97	0.99	0.22	6.15	0.97	0.26
	DTW classic	3.6	0.99	0.6	2.88	1	0.3	2.94	0.99	0.28
	DTW improved	3.37	0.99	0.54	2.88	0.99	0.33	2.83	0.99	0.24
Subject 4	no DTW	3.62	0.98	0.51	3.9	0.99	0.56	2.25	0.99	0.66
	DTW classic	2.66	0.99	0.58	1.72	1	0.67	1.84	1	0.59
	DTW improved	1.54	1	0.57	1.41	1	0.66	1.63	1	0.75
Subject 5	no DTW	4.38	0.97	0.66	5.97	0.96	0.19	4.13	0.98	0.26
	DTW classic	4.2	0.98	0.64	2.18	1	0.46	2.19	0.99	0.43
	DTW improved	3.27	0.99	0.46	2.92	0.99	0.3	2.21	0.99	0.4
Subject 6	no DTW	3.88	0.99	0.63	3.77	0.99	0.25	4.77	0.98	0.49
	DTW classic	3.39	0.99	0.63	2.77	0.99	0.33	1.56	1	0.89
	DTW improved	1.64	1	0.81	2.28	1	0.48	2.09	1	0.59
Subject 7	no DTW	7.77	0.86	0.69	4.73	0.98	0.25	10.1	0.9	0.27
	DTW classic	8.97	0.83	0.52	3.68	0.99	0.16	3.35	0.99	0.19
	DTW improved	3.36	0.99	0.68	3.17	0.99	0.21	2.84	0.99	0.19
Subject 8	no DTW	4.67	0.97	0.48	3.33	0.99	0.29	8.52	0.94	0.24
	DTW classic	4.05	0.98	0.46	2.57	0.99	0.44	2.26	0.99	0.46
	DTW improved	1.87	1	0.64	1.35	1	0.65	2.29	0.99	0.49
Subject 9	no DTW	5.91	0.95	0.41	8.33	0.93	0.23	5.53	0.97	0.31
	DTW classic	3.81	0.99	0.28	3.43	0.99	0.27	3.52	0.99	0.37
	DTW improved	3	0.98	0.42	2.91	0.99	0.52	2.65	1	0.49
Subject 10	no DTW	4.66	0.96	0.24	5.4	0.98	0.29	9.62	0.91	0.17
	DTW classic	3.82	0.98	0.22	2.66	0.99	0.27	2.34	0.99	0.31
	DTW improved	3.6	0.98	0.09	2.97	0.99	0.21	2.59	0.99	0.35
Average	no DTW	4.71 (1.46)	0.96 (0.04)	0.4 (0.18)	5.09 (1.41)	0.98 (0.02)	0.28 (0.1)	6.21 (2.53)	0.96 (0.03)	0.31 (0.14)
by speeds	DTW classic	4.1 (1.71)	0.97 (0.05)	0.38 (0.14)	2.97 (0.73)	0.99 (0)	0.35 (0.14)	2.61 (0.64)	0.99 (0)	0.41 (0.2)
[mean (std)]	DTW improved	2.74 (0.84)	0.99 (0.01)	0.51 (0.19)	2.63 (0.67)	0.99 (0)	0.41 (0.16)	2.59 (0.6)	0.99 (0)	0.5 (0.17)
Average		RMSE (°)			CC			SPM		
by subjects	no DTW	5.33 (2.01)			0.97 (0.03)			0.36 (0.18)		
and speeds	DTW classic	3.23 (1.32)			0.98 (0.03)			0.38 (0.17)		
[mean (std)]	DTW improved	2.65 (0.73)			0.99 (0.01)			0.48 (0.22)		

Table 1: Quantitative results of RMSE, CC and SPM for all the subjects and exercise speeds obtained using without DTW, with the classical and with the improved version of the DTW, respectively. The SPM represents the proportion of samples along the cycle which satisfy the statistical significance test.

Journal Pre-proofs

Journal Pre-proofs

Table 1 compares the results obtained without DTW, and using the classical or the improved DTW. The last row shows that the proposed technique reaches a lower RMSE (2.65°), the Correlation improves (0.99) and the SPM increases (0.48). The superior performance of the proposed method with respect to second most performant approach are statistically illustrated in Figure 4, and the p-values are significant (< 0.01) for all the metrics.

Regarding the angular error and bias, a mean RMSE value of 2.65° (0.731°) is obtained. This value corresponds to a 5.61% of the total range of movement (62.74°) showing that the amplitude of the bias between the measurement is low. Observing the average RMSE by exercise speeds, the results are comparable and are not dependent on the speed scenario as confirmed by the ANOVA tests (p-values: 0.76 for $RMSE_{sp1} vs\ RMSE_{sp2}$,0.68 for $RMSE_{sp1} vs\ RMSE_{sp3}$, 0.91 for $RMSE_{sp2} vs\ RMSE_{sp3}$, respectively).

Regarding the global waveform similarity, an average CC of 0.99 (0.01) is obtained. This value indicates that in all the cases there is a faithful matching between the shape of the curves.

With respect to the local waveform similarity, the SPM represents, per each point of the stride cycle, the similarity between the two waveforms. Figure 5 allow to assess in which part of the cycle the similarity between the two signal is higher.

The percentage of p-values above the threshold varies from 18% to 80% (see Figure 5) along the stride cycle. Then, if we study the variability among cases (varying the subject and exercise speed), the SPM reaches an average value of 48% (22%).

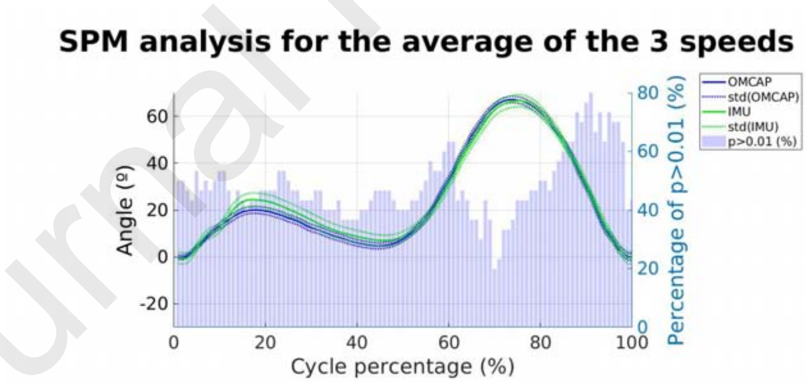

Figure 5: Gait profiles (blue and green solid lines) superimposed to the statistical results (p-values), averaged for all the subjects and exercise speeds. The left axis represents the angle acquired using the two systems.The time-wise percentage of p-values above the 0.01 threshold per each phase of the stride cycle is represented by a blue histogram (right axis).

Finally, to assess qualitatively the results, Figure 6 shows some exemplary cases of IMU and OMCAP signals aligned used the proposed technique. Each row of Figure 6 illustrates cases showing good, average and poor performances, while each column corresponds to a different exercise velocity. In the first row

Journal Pre-proofs

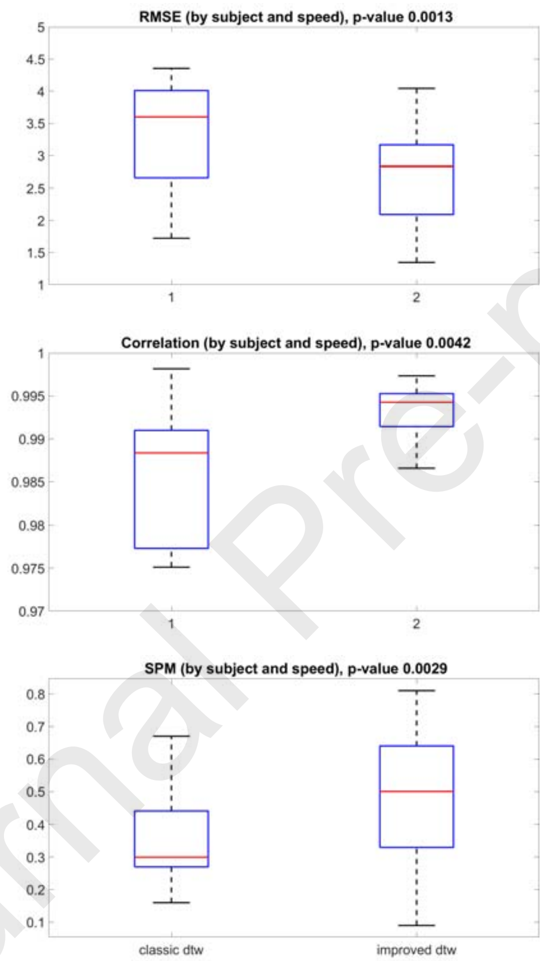

Figure 4: Statistical comparison between the classical and the improved DTW alignment. The boxplot reports the RMSE, CC and SPM percentage for all the subjects and exercise speeds, respectively. The p-value obtained by the ANOVA analysis is reported as title of each figure.

Journal Pre-proofs

Journal Pre-proofs

(a), it can be appreciated how, after the alignment, the acquisitions performed using the IMU sensor matches the OMCAP measurement along the whole cycle. The RMSE obtained in these cases is lower than 2°, indicating an excellent performance. In the second row (b) three cases having average performances, are illustrated. In this case, at specific phases of the cycle, it can be observed differences between the two acquisitions. However, in average, the IMU measurements are substantially accurate. Finally, in the third row (c) higher errors are present during segments of the cycle, particularly in the first half of the cycle or in the maximum peak. These curves correspond to the cases having an RMSE of 6° in Table 1.

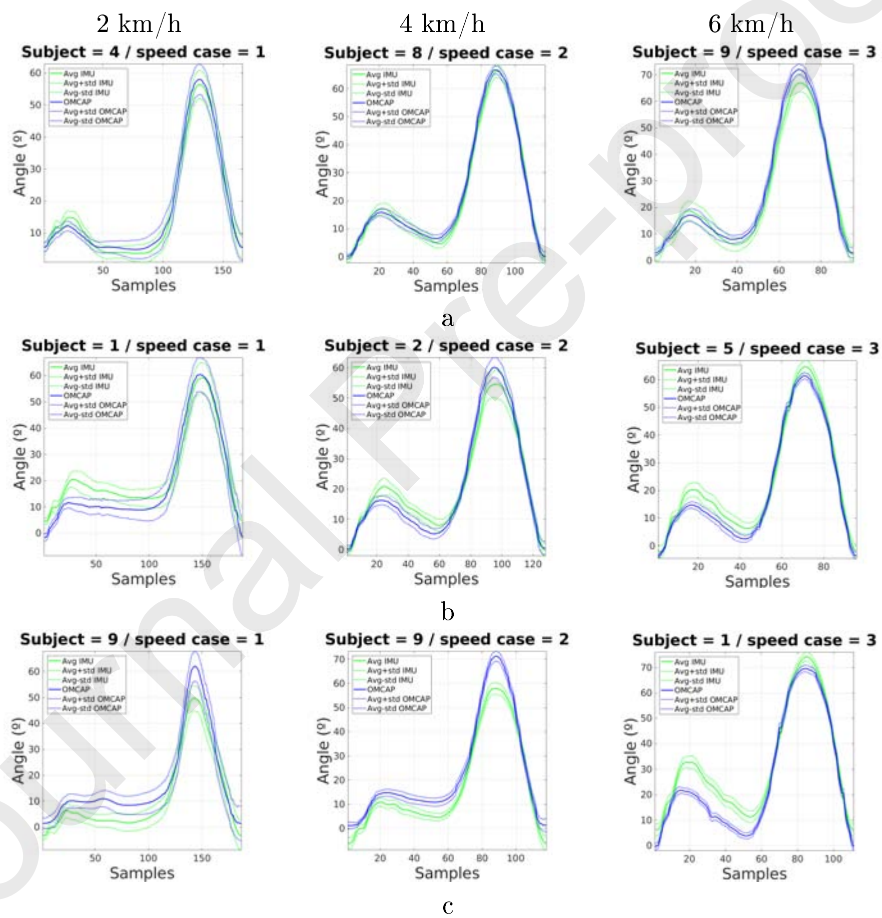

Figure 6: Results of signal comparisons from different subjects and speeds. Each column corresponds to a different experiment velocity, while on each row, exemplar curve representing a) a good b) average and c) poor agreement between the measurements are shown, respectively.

Journal Pre-proofs

Journal Pre-proofs

4. Conclusion

This study aims at introducing a pipeline for the non-rigid alignment of gait signals. In this study IMU and OMCAP acquisitions are aligned using, for the first time in gait analysis, a modified version of the DTW algorithm. As illustrated in Section 2.2, the modification of the classical DTW algorithm introduced in this paper allows obtaining a smoother matching between the signals, hence a more faithful signal synchronization.

The errors measured between IMU and OMCAP signals are in line with the bibliography, reaching a mean RMSE value of 2.65° (0.73°) and an average CC value of 0.99 (0.01). Such results, show that IMU devices may be considered as a cheaper, lighter and simpler alternative to OMCAP systems.

As a novelty, the SPM analysis conducted allows quantifying the measurement performances of the IMU in a phase-wise way. Scores obtained range from 18% to 80% along the gait cycle with an average of 48% (22%).

As a final remark, in this study, we are considering the OMCAP system as the gold standard, even if the system itself has an intrinsic measurement error (which is not declared by the producer). It also has to be contemplated that the knee considered as a pure hinge joint is an acceptable simplification for healthy subjects but also a limitation for expanding this work to pathological subjects.

Acknowledgments

RTI2018-095232-B-C21, 2017 SGR 1742, NEOTEC-SNEO-20171132 and 811755 – ReHub –2018-2020/H2020-SMEInst.

Castañeda, J., Ruiz-Olaya, A., Lara-Herrera, C., Roldán, F., 2017. Knee joint angle monitoring system based on inertial measurement units for human gait analysis, in: VII Latin American Congress on Biomedical Engineering CLAIB 2016, Bucaramanga, Santander, Colombia, October 26th-28th, 2016, Springer. pp. 690–693.

Cooper, G., Sheret, I., McMillian, L., Siliverdis, K., Sha, N., Hodgins, D., Kenney, L., Howard, D., 2009. Inertial sensor-based knee flexion/extension angle estimation. Journal of biomechanics 42, 2678–2685.

Cuesta-Vargas, A.I., Galán-Mercant, A., Williams, J.M., 2010. The use of inertial sensors system for human motion analysis. Physical Therapy Reviews 15, 462–473.

Cutti, A.G., Ferrari, A., Garofalo, P., Raggi, M., Cappello, A., Ferrari, A., 2010. Outwalk: a protocol for clinical gait analysis based on inertial and magnetic sensors. Medical & biological engineering & computing 48, 17.

Deluzio, K.J., Wyss, U.P., Zee, B., Costigan, P.A., Serbie, C., 1997. Principal component models of knee kinematics and kinetics: normal vs. pathological gait patterns. Human Movement Science 16, 201–217.

Journal Pre-proofs

Journal Pre-proofs

Dobson, F., Morris, M.E., Baker, R., Graham, H.K., 2007. Gait classification in children with cerebral palsy: a systematic review. Gait & posture 25, 140–152.

Donovan, K.J., Kamnik, R., Keeffe, D.T., Lyons, G.M., 2007. An inertial and magnetic sensor based technique for joint angle measurement. Journal of biomechanics 40, 2604–2611.

El-Gohary, M., McNames, J., 2015. Human joint angle estimation with inertial sensors and validation with a robot arm. IEEE Transactions on Biomedical Engineering 62, 1759–1767.

Engelhard, M.M., Dandu, S.R., Lach, J.C., Goldman, M.D., Patek, S.D., 2015. Toward detection and monitoring of gait pathology using inertial sensors under rotation, scale, and offset invariant dynamic time warping, in: Proceedings of the 10th EAI International Conference on Body Area Networks, ICST (Institute for Computer Sciences, Social-Informatics and Telecommunications Engineering). pp. 269–275.

Favre, J., Jolles, B., Aissaoui, R., Aminian, K., 2008. Ambulatory measurement of 3d knee joint angle. Journal of biomechanics 41, 1029–1035.

Favre, J., Luthi, F., Jolles, B., Siegrist, O., Najafi, B., Aminian, K., 2006. A new ambulatory system for comparative evaluation of the three-dimensional knee kinematics, applied to anterior cruciate ligament injuries. Knee Surgery, Sports Traumatology, Arthroscopy 14, 592–604.

Ferrari, A., Cutti, A.G., Garofalo, P., Raggi, M., Heijboer, M., Cappello, A., Davalli, A., 2010. First in vivo assessment of outwalk: a novel protocol for clinical gait analysis based on inertial and magnetic sensors. Medical & biological engineering & computing 48, 1.

J.., F.K., 2007. Statistical Parametric Mapping: The Analysis of Functional Brain Images. Elsevier/Academic Press. , Ashburner J. T., Kiebel S. J., Nichols T. E. and Penny, W. D.

Keogh, E., Ratanamahatana, C.A., 2005. Exact indexing of dynamic time warping. Knowledge and information systems 7, 358–386.

Knoll, Z., Kiss, R.M., Kocsis, L., 2004. Gait adaptation in acl deficient patients before and after anterior cruciate ligament reconstruction surgery. Journal of Electromyography and Kinesiology 14, 287–294.

Koller, W.C., Trimble, J., 1985. The gait abnormality of huntington's disease. Neurology 35, 1450–1450.

Müller, M., 2007. Dynamic Time Warping. In: Information Retrieval for Music and Motion. Springer, Berlin, Heidelberg. Springer, Berlin, Heidelberg.

Journal Pre-proofs

Journal Pre-proofs

Noort, J.C., Ferrari, A., Cutti, A.G., Becher, J.G., Harlaar, J., 2013. Gait analysis in children with cerebral palsy via inertial and magnetic sensors. Medical & Biological Engineering & Computing 51, 377. URL: http://dx.doi.org/10.1007/s11517-012-1006-5, doi:10.1007/s11517-012-1006-5.

Paquet, J., Auvinet, B., Chaleil, D., Barrey, E., 2003. Analysis of gait disorders in parkinson's disease assessed with an accelerometer. Revue neurologique 159, 786–789.

Pataky, T.C., Caravaggi, P., Savage, R., Parker, D., Goulermas, J.Y., Sellers, W.I., Crompton, R.H., 2008. New insights into the plantar pressure correlates of walking speed using pedobarographic statistical parametric mapping (pspm). Journal of biomechanics 41, 1987–1994.

Pataky, T.C., Robinson, M.A., Vanrenterghem, J., 2013. Vector field statistical analysis of kinematic and force trajectories. Journal of biomechanics 46, 2394–2401.

Picerno, P., Cereatti, A., Cappozzo, A., 2008. Joint kinematics estimate using wearable inertial and magnetic sensing modules. Gait & posture 28, 588–595.

Robinson, M.A., Vanrenterghem, J., Pataky, T.C., 2015. Statistical parametric mapping (spm) for alpha-based statistical analyses of multi-muscle emg time-series. Journal of Electromyography and Kinesiology 25, 14–19.

Roetenberg, D., Luinge, H., Slycke, P., 2009. Xsens mvn: full 6dof human motion tracking using miniature inertial sensors. Xsens Motion Technologies BV, Tech. Rep 1.

Seel, T., Raisch, J., Schauer, T., 2014. Imu-based joint angle measurement for gait analysis. Sensors 14, 6891–6909.

Sessa, S., Zecca, M., Lin, Z., Bartolomeo, L., Ishii, H., Takanishi, A., 2013. A methodology for the performance evaluation of inertial measurement units. Journal of Intelligent & Robotic Systems 71, 143–157.

Takeda, R., Tadano, S., Natorigawa, A., Todoh, M., Yoshinari, S., 2009. Gait posture estimation using wearable acceleration and gyro sensors. Journal of biomechanics 42, 2486–2494.

Tao, W., Liu, T., Zheng, R., Feng, H., 2012. Gait analysis using wearable sensors. Sensors 12, 2255–2283.

Vanrenterghem, J., Gormley, D., Robinson, M., Lees, A., 2010. Solutions for representing the whole-body centre of mass in side cutting manoeuvres based on data that is typically available for lower limb kinematics. Gait & posture 31, 517–521.

Journal Pre-proofs

Journal Pre-proofs

Watanabe, T., Saito, H., Koike, E., Nitta, K., 2011. A preliminary test of measurement of joint angles and stride length with wireless inertial sensors for wearable gait evaluation system. Computational intelligence and neuroscience 2011, 6.

Zhou, S., Fei, F., Zhang, G., Mai, J.D., Liu, Y., Liou, J.Y., Li, W.J., 2014. 2d human gesture tracking and recognition by the fusion of mems inertial and vision sensors. IEEE Sensors Journal 14, 1160–1170.

Journal Pre-proofs